Ruderman-Kittel-Kasuya-Yosida–like Ferromagnetism in Mn_xGe_{1-x}

Yu-Jun Zhao, Tatsuya Shishidou, and A. J. Freeman

Department of Physics & Astronomy, Northwestern University, Evanston, Illinois 60208

(Received 9 August 2002; published 31 January 2003)

The nature and origin of ferromagnetism in magnetic semiconductors is investigated by means of highly precise electronic and magnetic property calculations on Mn_xGe_{1-x} as a function of the location of Mn sites in a large supercell. Surprisingly, the coupling is not always ferromagnetic (FM), even for large Mn-Mn distances. The exchange interaction between Mn ions oscillates as a function of the distance between them and obeys the Ruderman-Kittel-Kasuya-Yosida analytic formula. The estimated Curie temperature is in good agreement with recent experiments, and the estimated effective magnetic moment is about $1.7\mu_B$/Mn, in excellent agreement with the experimental values, $(1.4–1.9)\mu_B$/Mn.

DOI: 10.1103/PhysRevLett.90.047204 PACS numbers: 75.50.Pp, 71.55.Cn, 75.30.Hx

Semiconductor devices based on the control and manipulation of electron spin have recently attracted great attention, including Mn doped III-V [1], group IV [2], and chalcopyrite [3,4] semiconductors. The origin of the ferromagnetism in magnetic semiconductors is under intense discussion [5], with many mechanisms proposed, including the Ruderman-Kittel-Kasuya-Yosida (RKKY) model [6], and double resonance mechanism [7]. Recently, a number of investigators have noticed that the disorder of Mn site locations might play an important role [5,8–10]: disorder was found to enhance the ferromagnetic (FM) transition temperature both in the mean-field approximation and from an analysis of the zero-temperature spin stiffness [8,9]. Experimentally, it is also well known that the electronic and magnetic properties are strongly affected by the temperature or duration of annealing [10–12]. For example, large variations of T_C, from 49 to 111 K in $Ga_{1-x}Mn_xAs$ at $x =$ 6%–8%, were found when annealing at different temperatures in a narrow temperature range, from 282 to 350 K [10]. For Mn_xGe_{1-x}, T_C was found to be as high as 274 K in a very recent work [13], in contrast with up to 116 K found previously. Recent experimental work [2] demonstrated the control of FM order of Mn_xGe_{1-x} through the application of a ± 0.5 V gate voltage, showing the potential application of Mn_xGe_{1-x} in microelectronic technology.

To gain insight into the magnetic interaction responsible for ferromagnetism observed in Mn_xGe_{1-x}, we have carried out highly precise all-electron full-potential linearized augmented plane wave (FLAPW) [14] calculations on large supercells as a function of Mn-Mn distances for different Mn site locations. Here we report that the coupling between Mn atoms is not always ferromagnetic even for large Mn distances. The magnetic order in Mn_xGe_{1-x} strongly depends on the Mn site locations due to a RKKY-like interaction between the localized Mn ions. Our results serve to explain the experimental effective magnetic moments and the observed large range of Curie temperature in Mn_xGe_{1-x}. They also indicate that a higher Mn concentration enhances the exchange interactions and thus the Curie temperature.

The FLAPW method [14], one of the most accurate *ab initio* methods, is employed with no artificial shape approximation for the wave functions, charge density, and potential. The core states are treated fully relativistically and the valence states are treated semirelativistically (i.e., without spin-orbit coupling) for both Ge and Mn. The muffin-tin radii are chosen as 2.20 a.u. for both types of atoms. An energy cutoff of 9.0 Ry is employed for the APW basis to describe the wave functions in the interstitial region, and an energy cutoff of 81.0 Ry is used for the star functions depicting the charge density and potential. When the energy cutoff for the APW basis is increased to 12.96 Ry, the total energy difference between the antiferromagnetic (AFM) state and the corresponding FM state changes only within 3 meV/Mn. Following the Monkhorst-Pack scheme, a $3 \times 3 \times 3$ k mesh, is adopted [15]. The energy differences between FM and AFM states change within 4 meV/Mn, when the k mesh is enhanced to $4 \times 4 \times 4$ or $5 \times 5 \times 5$, whereas the results with a $2 \times 2 \times 2$ k mesh are not well converged, and even give an incorrect magnetic ground state for some of these systems. The generalized gradient approximation functional of Perdew, Burke, and Ernzerhof [16] is employed for the calculations in order to get a better description for the Mn atom. The lattice constant of pure Ge, i.e., 5.658 Å, is used for Mn concentrations from 3.1% to 6.3%, since it was found to change only within 0.46% up to $x = 6.3\%$ [13].

We employed a $2 \times 2 \times 2$ a^3 supercell (a is the cubic lattice constant), with 62 Ge atoms and 2 Mn atoms, to simulate the effect of local disorder of the Mn distributions, with Mn-Mn distances ranging from 2.45 to 9.80 Å. All six cases are described in Table I, with a system notation for each case, consisting of three digits following N to represent (x, y, z) coordinates in units of $a/4$ of the second Mn (the first is at the origin). The total energy results indicate that the Mn pair does not prefer either the nearest neighbor ($N111$ case) or the uniform distribution with the largest Mn-Mn separation distance ($N444$ case).

TABLE I. The FLAPW calculated total energy (relative to the lowest energy $N440$ FM case), the AFM and FM energy difference, for the different Mn locations from the $Ge_{62}Mn_2$ supercell. One Mn is put at (0, 0, 0), while the other is listed in the table. The expression of exchange constants for the AFM and FM energy difference is listed in the last column.

System	Mn2 position (a)	Mn-Mn dist (Å)	E_{FM} (meV/Mn)	E_{AFM} (meV/Mn)	$E_{AFM} - E_{FM}$ (meV/Mn)	$= \sum J(r)$
$N111$	(1/4, 1/4, 1/4)	2.45	290.3	2.7	−287.6	J_{111}
$N220$	(1/2, 1/2, 0)	4.00	12.2	93.6	81.4	J_{220}
$N400$	(1, 0, 0)	5.66	67.9	45.5	−22.4	$2J_{400}$
$N224$	(1/2, 1/2, 1)	6.93	75.9	68.8	−7.1	$2J_{224}$
$N440$	(1, 1, 0)	8.00	0	103.1	103.1	$4J_{440}$
$N444$	(1, 1, 1)	9.80	106.8	69.3	−37.5	$8J_{444}$

Instead, the FM $N440$ case with the Mn-Mn separation of 8.0 Å has the lowest energy. Surprisingly, the Mn_xGe_{1-x} is not always ferromagnetic even at large Mn-Mn distances (see Table I). For the nearest neighbor situation (case $N111$), AFM is strongly preferred, as found in other calculations [2]. However, the AFM states for $N400$ and $N444$ are clearly lower than the FM state by energies of 22.4 and 37.5 meV, respectively, which are larger than the error (~ 10 meV/Mn) of our calculations. Therefore, the mechanism for the ferromagnetism in Mn_xGe_{1-x} is not simply from the competition between a long-range FM interaction and a short-range AFM interaction, as supposed in Ref. [2]. We show that the magnetic interaction in Mn_xGe_{1-x} follows the RKKY analytic formula.

Our first principles calculations listed in Table I clearly show the oscillation of the AFM and FM energy difference as a function of the Mn-Mn distance. To understand this behavior, we express the energy difference between the AFM state and the FM state with the Heisenberg model, where the spin interaction energy in a supercell, Ω, can be expressed as

$$E = -\frac{1}{2}\sum_{j_\alpha \neq i}\sum_{i\in\Omega} J(\mathbf{r}_{i,j_\alpha})\,\mathbf{S}_i \cdot \mathbf{S}_{j_\alpha}. \quad (1)$$

Here α represents all the supercells expanded in the solid, and $\mathbf{S}_i$, $\mathbf{S}_j$ denote the localized magnetic moments. The factor of $\frac{1}{2}$ is added because the interaction is shared by two atoms. When defined with the convention $|\mathbf{S}| = 1$, the energy difference between the AFM and FM aligned $Ge_{62}Mn_2$ supercells for each Mn atom may be expressed as

$$\Delta E_{ex} = \sum_{\alpha_1,\alpha_2,\alpha_3} J(x_1 + 8\alpha_1, x_2 + 8\alpha_2, x_3 + 8\alpha_3). \quad (2)$$

Here (x_1, x_2, x_3) represents the coordinates of the second Mn in units of $a/4$, and the lattice vectors (with length $= 2a$) in three directions are replaced with $8\alpha_1$, $8\alpha_2$, and $8\alpha_3$ in units of $a/4$, and α_1, α_2, and α_3 are integers. For example, in the $N400$ case, Eq. (2) can be written as $\Delta E_{ex} = J(4, 0, 0) + J(-4, 0, 0)$ if $J(r)$ is cut off beyond $r = 2a$. Since $J(4, 0, 0)$ and $J(-4, 0, 0)$ are equivalent, they are simplified into $2J_{400}$ in Table I. The calculated $J(r)$'s are displayed as diamond dots in Fig. 1. It is important to point out that $J(r)$ may be understood as the energy required to flip two aligned localized magnetic moments at a distance, r.

On the other hand, according to RKKY theory [17], the interaction between two localized moments through the induced spin density has the form of

$$\mathcal{H} = -\frac{J^2}{g^2\mu_B^2 V}\sum_{\mathbf{q}} \chi(\mathbf{q}) e^{i\mathbf{q}\cdot\mathbf{r}} \mathbf{S}_\alpha \cdot \mathbf{S}_\beta. \quad (3)$$

Here J is the exchange integral between conduction electrons and the electron localized at the impurity, and $\chi(\mathbf{q})$ is the magnetic susceptibility of the conduction electrons. It is well known that if $\chi(\mathbf{q})$ is treated as for free electrons then the RKKY Hamiltonian could be rewritten as

$$\mathcal{H} \propto \sum_{\mathbf{q}} \chi(\mathbf{q}) e^{i\mathbf{q}\cdot\mathbf{r}} \propto [\sin(2k_F r) - 2k_F r\cos(2k_F r)]/r^4, \quad (4)$$

where k_F is the Fermi wave vector corresponding to the average density $\bar{\rho}$. Consider now the RKKY Hamiltonian for two situations, $\mathbf{S}_\alpha$, $\mathbf{S}_\beta$, with parallel and opposite directions, which will have the same expression as in

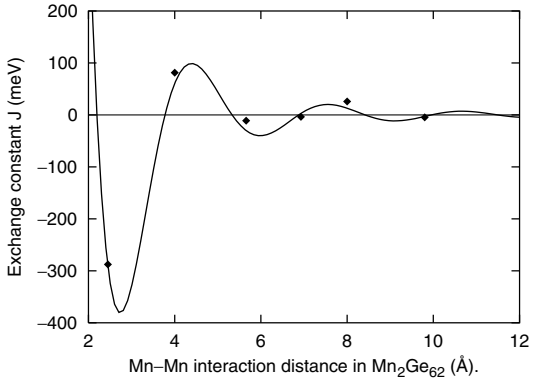

FIG. 1. The exchange interaction, J_n, for the Mn atoms versus their distance in Mn_xGe_{1-x}, where the J_n's are defined with the convention $|\mathbf{S}| = 1$. The solid line is the RKKY model fitted with $k_F = 1.02$ Å^{-1}.

Eq. (4) except for their signs [18]. Therefore, the energy difference between the AFM state and the FM state of the two localized moment systems, which is exactly the $J(r)$ discussed above, is also proportional to the right-hand side of Eq. (4).

We now fit the calculated exchange interaction $J(r)$ with Eq. (4), taking k_F as a parameter. The fitted curve shown in Fig. 1 as the solid line shows excellent agreement between the calculated $J(r)$'s and the RKKY model. It is not appropriate to estimate k_F from the hole concentrations because the holes are mostly contributed by Mn $3d$ and nearby Ge $4p$ electrons, and thus are localized at Mn sites. From Fig. 2(b), it is seen that the Ge $4p$ partial density of states (DOS) decreases rapidly as the Ge atom goes away from the Mn, which indicates that the "free" charges have a much larger density around the Mn.

The spin density for the FM and AFM $N440$ cases shown in Fig. 3 clearly indicates that the magnetic moments are localized at Mn sites. At Ge sites that are nearest neighbors to Mn the magnetic moment within their muffin-tin spheres is about $0.06\mu_B$ ($0.05\mu_B$ for the AFM case), has an opposite spin direction to that of nearby Mn, and decreases rapidly to zero as the distance increases. That the Ge $4s$ and $4p$ electrons prefer AFM alignment to the nearby Mn $3d$ is similar to the As $4s$ and $4p$ in (Ga, Mn)As [19]. The total DOS of FM $N440$, shown in Fig. 2(a), indicates that the system is half metallic — consistent with the average integer magnetic moments of $3\mu_B$/Mn. Figure 2(b) shows that the nearby Ge $4p$ is hybridized with the Mn $3d$, and the hybridization decreases rapidly as the distance to Mn increases.

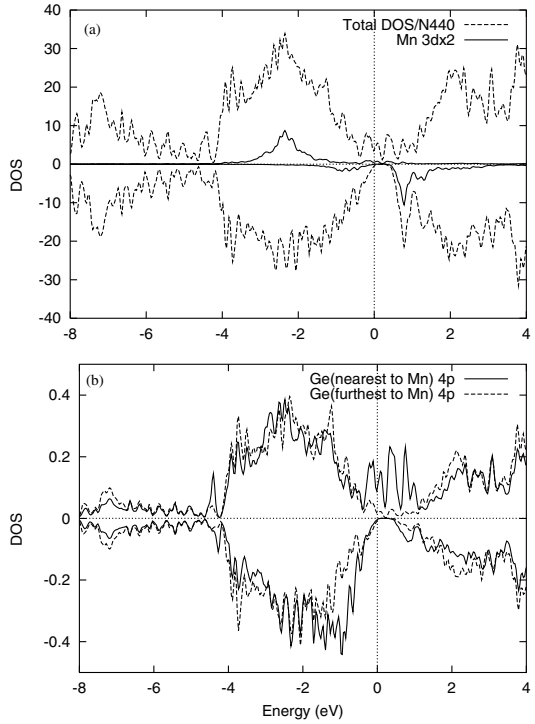

FIG. 2. The total DOS and projected Mn $3d$ and Ge $4p$ DOS of the $N440$ FM case in $Ge_{62}Mn_2$, with Gaussian broadening technique with a parameter of 0.05 eV. Spin up and spin down are represented with positive and negative images, respectively. The distance of the nearest Ge to Mn is 2.45 Å while it is 6.93 Å for the furthest Ge atom.

Despite much effort, the optimum way to estimate the Curie temperature is still an open question. As done for the $CuGa_{1-x}Mn_xSe_2$ system [20], we employ Monte Carlo simulation results for $Cd_{1-x}Mn_xTe$, which has the zinc-blende structure [21], namely $T_C = 0.447|J_1|$, where J_1 is the exchange constant for the nearest neighbor interaction between local magnetic ions. The estimated T_c is ~134 K for the energetically preferred $N440$ case (with $J_1 = 25.8$ meV), and it could be up to ~400 K for Mn atoms located as in the $N220$ case (with $J_1 = 81.4$ meV), and so appear to be in good agreement with the experimental results, 116 [2] and 274 K[13], obtained by different groups. The larger T_C for the $N220$ case confirms results from the mean-field approximation and an analysis of the zero-temperature spin stiffness that Mn disorder may enhance the ferromagnetic transition temperature [8,9].

In addition, the effective magnetic moment in Mn_xGe_{1-x} may be estimated from the calculated total energies which mostly lie within 100 meV/Mn higher than the N440 FM case, as listed in Table I. Considering that the growth/annealing temperature for Mn_xGe_{1-x} sample synthesis is about 340 K [2], i.e., 29 meV, most of the Mn site locations are competitive for occupation. The calculated magnetic moment is $3.0\mu_B$ per Mn for all systems except for the FM $N111$ case ($3.12\mu_B$ per Mn). Now, the saturation magnetization obtained from the experimental magnetization loops is up to 30 emu/cm^3 for $Mn_{0.02}Ge_{0.98}$, corresponding to $(1.4–1.9)\mu_B$/Mn if all Mn atoms contribute equally [2]. This means that only ~50% Mn are magnetically active if each Mn atom has the theoretical moment of $3\mu_B$. Since the Mn locations are rather random due to their competitive total energies and the magnetic moments of Mn are not "active" in some cases, like $N111$ and $N400$, due to the AFM state being preferred, this may explain why the experimental magnetic moments are much

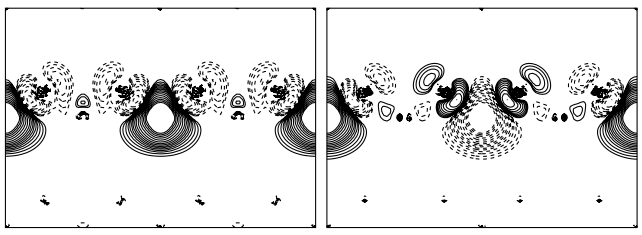

FIG. 3. The spin density of the $N440$ case in $Ge_{62}Mn_2$ for both FM (left) and AFM (right) configurations. The solid (dashed) lines represent spin up (down) density with $\rho = 0.0005 \times 2^{(n-1)/2} e/\text{bohr}^3$. Here n represents the nth contour line from the lowest density zone.

TABLE II. The FLAPW calculated total energy (relative to the lowest energy $N220$ FM case) of the $Ge_{30}Mn_2$ supercell with the same K_{max} and G_{max} as $Ge_{62}Mn_2$. The k mesh of $3 \times 3 \times 6$, equivalent to the calculations of $Ge_{62}Mn_2$, is used. One Mn is put at the (0, 0, 0) position; the other Mn position is listed in the table.

System	Mn2 position (a)	Mn-Mn dist (Å)	E_{FM} (meV/Mn)	$E_{AFM} - E_{FM}$ (meV/Mn)	$= \sum \alpha_n J_n$
$N111$	(1/4, 1/4, 1/4)	2.45	310.8	−242.7	$J_{111} + J_{113} + J_{115}$
$N220$	(1/2, 1/2, 0)	4.00	0	123.3	$J_{220} + 2J_{224}$
$N400$	(1, 0, 0)	5.69	4.7	104.7	$2J_{400} + 4J_{440}$
$N440$	(1, 1, 0)	8.00	40.1	81.2	$4J_{440} + 8J_{444}$

smaller than the theoretical values. As a crude estimate, we assume that the Mn are distributed in the six cases listed in Table I [22] with relative weights given by a Boltzmann factor, $\exp(-\Delta E_i/KT)$. The calculated effective magnetic moment, $1.7\mu_B$/Mn (for growth temperature of 340 K), is in excellent agreement with experiment.

In order to investigate the effect of Mn concentration on the magnetic properties in Mn_xGe_{1-x}, a supercell of $Ge_{61}Mn_3$ was also employed, with three Mn atoms located at (0, 0, 0), (2, 2, 0), and (4, 4, 0) in units of $a/4$. The energy difference between the FM state and the AFM state [with the Mn at (2, 2, 0) AFM aligned with the other two] is 222.4 meV for the 64-atom supercell. This energy difference may be expressed as $2J_{220}$ when cutting off the interactions beyond 12 Å, and so J_{220} is 111.2 meV, which is much larger than the 81.4 meV value of J_{220} for $Ge_{62}Mn_2$. Therefore, the $J(r)$'s are getting larger as the Mn concentration increases, which is in agreement with the fact that T_C increases as Mn concentration increases. The calculated results for Mn_xGe_{1-x} at $x = 6.3\%$ also support this conclusion, as seen from the total energies for several Mn configurations in a $2 \times 2 \times 1\ a^3$ supercell of $Ge_{30}Mn_2$ listed in Table II. In the last column of Table II, the energy difference between the AFM state and the FM state is expressed in terms of the $J(r)$'s. It is not surprising that the $N400$ case in $Ge_{30}Mn_2$ is FM favored since it includes J_{440} in addtion to J_{400}. Since we are not able to obtain these $J(r)$'s for $x = 6.3\%$ from Table II, we use the $J(r)$ values obtained for $x = 3.1\%$; the calculated energy difference between the AFM state and the FM state is now much larger than the value from the $J(r)$ expressions. For example, the calculated energy difference for $N220$, 123.3 meV, is much larger than that from the $J(r)$'s ($J_{220} + 2J_{224} = 74.2$ meV). This clearly confirms that the exchange interaction will be much enhanced as the Mn concentration increases, and thus the Curie temperature will also be increased if it were possible to increase the Mn concentration.

This work was supported by DARPA-ONR and grants of computer time at the NAVO and ERDC Supercomputing Centers.

[1] H. Ohno, Science **281**, 951 (1998).
[2] Y. D. Park *et al.*, Science **295**, 651 (2002).
[3] G. A. Medvedkin *et al.*, Jpn. J. Appl. Phys. **39**, L949 (2000).
[4] Y.-J. Zhao, S. Picozzi, A. Continenza, W. T. Geng, and A. J. Freeman, Phys. Rev. B **65**, 094415 (2002).
[5] P. Korzhavyi *et al.*, Phys. Rev. Lett. **88**, 187202 (2002).
[6] T. Dietl, H. Ohno, J. Cibert, and D. Ferrand, Science **287**, 1019 (2000).
[7] J. Inoue, S. Nonoyama, and H. Itoh, Phys. Rev. Lett. **85**, 4610 (2000).
[8] M. Berciu and R. N. Bhatt, Phys. Rev. Lett. **87**, 107203 (2001).
[9] A. L. Chudnovskiy and D. Pfannkuche, Phys. Rev. B **65**, 165216 (2002).
[10] K. M. Yu *et al.*, Phys. Rev. B **65**, 201303 (2002).
[11] T. Hayashi, Y. Hashimoto, S. Katsumoto, and Y. Iye, Appl. Phys. Lett. **78**, 1691 (2001).
[12] S. J. Potashnik *et al.*, Appl. Phys. Lett. **79**, 1495 (2001).
[13] S. Cho *et al.*, Phys. Rev. B **66**, 033303 (2002).
[14] E. Wimmer, H. Krakauer, M. Weinert, and A. J. Freeman, Phys. Rev. B **24**, 864 (1981).
[15] H. J. Monkhorst and J. D. Pack, Phys. Rev. B **13**, 5188 (1976).
[16] J. P. Perdew, K. Burke, and M. Ernzerhof, Phys. Rev. Lett. **77**, 3865 (1996).
[17] R. M. White, *Quantum Theory of Magnetism* (McGraw-Hill, New York, 1970).
[18] Here we assumed that k_F for both FM and AFM states has the same value, which is reasonable because their calculated total charge density has no remarkable difference.
[19] Y.-J. Zhao, W. T. Geng, K. T. Park, and A. J. Freeman, Phys. Rev. B **64**, 035207 (2001).
[20] Y.-J. Zhao and A. J. Freeman, J. Magn. Magn. Mater. **246**, 145 (2002).
[21] H. T. Diep and H. Kawamura, Phys. Rev. B **40**, 7019 (1989).
[22] Of course, there are many more possible Mn locations in the 64-atom and larger supercells, but it is good enough to represent the real situation with the Mn-Mn distance ranging from 2.45 to 9.80 Å.